

Gold Cluster Carbonyls: Vibrational Spectroscopy of the Anions and the Effects of Cluster Size, Charge, and Coverage on the CO Stretching Frequency

André Fielicke,^{*,‡} Gert von Helden,[‡] Gerard Meijer,[‡] Benoit Simard,[§] and David M. Rayner^{*,§}

Fritz-Haber-Institut der Max-Planck-Gesellschaft, Faradayweg 4-6, D-14195 Berlin, Germany, and
Steacie Institute for Molecular Sciences, National Research Council, 100 Sussex Drive,
Ottawa, Ontario K1A 0R6, Canada

Received: October 13, 2005

We report the vibrational spectra of the carbonyl complexes of anionic gold clusters in the range of the CO stretching frequency as measured in the gas phase using IR multiple photon dissociation spectroscopy. The investigated complexes contain between 3 and 14 Au atoms and up to 7 CO ligands. Special attention is given to the complexes that exhibit saturation CO coverage as well as to the monocarbonyl species. In conjunction with data from the corresponding cationic complexes we quantify how the CO stretching frequency varies with the charge state of the gold cluster. Our results provide a size- and charge-dependent basis to interpret values of the CO stretching frequency measured for CO on deposited gold clusters in terms of the charge states of the clusters.

Introduction

The findings of Haruta¹ that nanometer sized gold particles are effective catalysts for oxidation reactions have triggered many studies to elucidate the origin of the enhanced reactivity of those nanoparticles. These studies are often focused on systems resembling “real” catalysts such as deposited gold clusters, nanocrystals, or films on metal oxide substrates. Investigations on gas-phase clusters allow for insights into reaction mechanisms and aid development of theory.

The charge state and the charge distribution are thought to play a central role in the reactivity of supported gold clusters. In the gas phase, the sensitivity to the charge state is well established. Here, for instance, distinct differences are found in the reactivity of cationic and anionic gold clusters with molecular oxygen, with the cationic clusters being much less reactive and a pronounced odd–even oscillation in the reactivity of the anions.² Accordingly it has been proposed that the gold species catalyzing the CO oxidation by O₂ could be an initially partially negatively charged cluster.^{3,4} On MgO surfaces such a charge transfer is suggested to originate from an interaction of the gold clusters with an oxygen vacancy (F-center). The presence of partially negatively charged gold clusters is also proposed for gold deposited on TiO₂.⁵ Depending on the substrate, positively polarized clusters can be identified as well.^{5,6} How this charging affects the reactivity of deposited nanosized gold particles is still under discussion.

Most of the information about the charge states of deposited metal particles is derived from the measurement of IR spectra of adsorbed CO. A comprehensive overview of vibrational frequencies found for CO adsorbed on Au particles is given in a review on the surface chemistry of catalysis by gold by Freund and co-workers.⁷ In these adsorbates the C–O bond strength and thereby its stretching frequency, $\nu(\text{CO})$, is sensitive to the

electron density on the metal center. For transition metals, the Blyholder model of σ -donation and π^* -back-donation provides a qualitative understanding of how the charge at the metal center relates to $\nu(\text{CO})$.⁸ An empirical, but more quantitative, approach to assessing the charge of supported clusters from $\nu(\text{CO})$ relies on baseline measurements of $\nu(\text{CO})$ in small isolated metal carbonyl species. This approach is originally based on low-temperature matrix studies of neutral, cationic, and anionic complexes of metal atoms with CO.⁹ A more reliable, size-selective approach is to base the calibration on gas-phase values of $\nu(\text{CO})$ of cluster complexes. For instance, we have recently demonstrated a strong, cluster-size dependence of $\nu(\text{CO})$ on the charge state for monocarbonyls of rhodium clusters, $\text{Rh}_n\text{CO}^{+/0/-}$, in the size range of $n = 3\text{--}15$.¹⁰ The so obtained $\nu(\text{CO})$ values can then be used to assign the charge of deposited clusters.

In this work we extend our earlier studies on the vibrational spectroscopy of cationic gold cluster carbonyls¹¹ to the anionic species. The kinetics of the reaction of anionic gold clusters with CO have been studied earlier.^{12,13} Whetten and co-workers have studied the formation of anionic gold cluster carbonyls $\text{Au}_n(\text{CO})_m^-$ and the occurrence of pronounced CO saturation numbers m_{sat} .^{14–16} Zhai and Wang have reported chemisorption saturation numbers for smaller clusters ($n = 2$ to 5) obtained from photoelectron spectroscopy (PES).¹⁷ In contrast to the cationic systems, the saturation stoichiometries are not easily explained by the underlying geometrical structures of the clusters. Here we use IR multiple photon dissociation (IR-MPD) spectroscopy to measure the vibrational spectra of gas-phase $\text{Au}_n(\text{CO})_m^-$ in the range of the $\nu(\text{CO})$ vibrations. We obtain information on the binding situation of the CO ligands in the anionic gold cluster carbonyls and discuss how the $\nu(\text{CO})$ values can be used as reference values of complexes with a defined charge state for comparison with other systems, e.g., deposited clusters.

Experimental Section

The methods we use to measure the IR-MPD spectra of metal cluster complexes have been described in detail earlier.^{10,11,18}

* Address correspondence to these authors. E-mail: david.rayner@nrc-cnrc.gc.ca, fielicke@fhi-berlin.mpg.de.

[‡] Fritz-Haber-Institut der Max-Planck-Gesellschaft.

[§] Steacie Institute for Molecular Science.

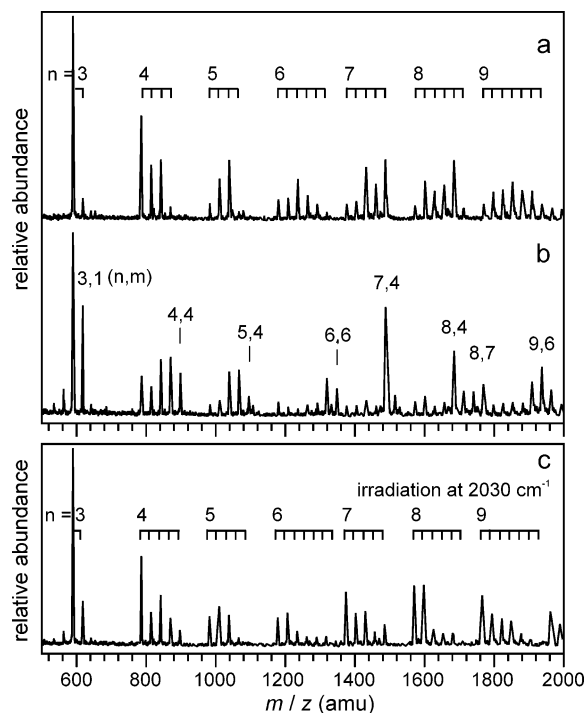


Figure 1. Mass spectra of anionic gold cluster carbonyls $\text{Au}_n(\text{CO})_m^-$; the numbers (n,m) are indicated. The upper trace (a) shows a mass spectrum of gold clusters Au_n^- , partially complexed with CO. The middle spectrum (b) is taken at higher $p(\text{CO})$ where saturation coverage is established. The lower spectrum (c) is obtained when the distribution shown in part b is irradiated at 2030 cm^{-1} .

Briefly, the clusters are produced by pulsed laser ablation. For complex formation, CO is introduced via a second pulsed valve into a short extension (flow reactor) attached to the cluster source. The molecular beam containing the gold cluster CO complexes is overlapped with a pulsed IR beam produced by the Free Electron Laser for Infrared eXperiments (FELIX).¹⁹ The overlap region is confined by an aperture that is placed in the molecular beam between the focus of the IR beam and the extraction region of a time-of-flight mass spectrometer. IR-MPD spectra are generated from mass spectra that are recorded as the FELIX wavelength is scanned incrementally. The IR light is produced by FELIX in macropulses of $7\text{ }\mu\text{s}$ duration, at a repetition rate of 5 Hz. Each macropulse consists of a 1 GHz train of micropulses of typically 2 ps duration. For the experiments reported here the macropulse energy was attenuated to $\sim 10\text{ mJ}$.

Results

Addition of CO in the flow reactor leads to formation of CO complexes of the anionic gold clusters. By varying the back-pressure and/or the opening time of the valve, the amount of complexation can be adjusted ranging from the monocarbonyls Au_nCO^- to a cluster size specific saturation composition. The upper mass spectrum in Figure 1 shows a distribution where for some cluster sizes saturation is already reached. An indication of saturation is an enhanced intensity at the saturated composition, e.g. $\text{Au}_7(\text{CO})_4^-$, and the absence of higher complexes. By adding more CO (middle trace) this saturation effect becomes more apparent. Enhanced intensities are found for cluster complexes with the compositions Au_3CO^- , $\text{Au}_4(\text{CO})_4^-$, $\text{Au}_5(\text{CO})_4^-$, $\text{Au}_6(\text{CO})_6^-$, $\text{Au}_7(\text{CO})_4^-$, $\text{Au}_8(\text{CO})_4^-$, $\text{Au}_9(\text{CO})_6^-$, and $\text{Au}_{10}(\text{CO})_6^-$ (Table 1). However, for the bigger clusters ($n \geq 7$) those compositions are not necessarily the limits of CO binding, but correspond to an intermediate saturation. CO

TABLE 1: Saturation Compositions of $\text{Au}_n(\text{CO})_m^-$ Complexes and CO Stretching Frequencies, $\nu(\text{CO})$ in cm^{-1} ,^a for the Saturated Complexes and for the Corresponding Monocarbonyl Complexes, Au_nCO^-

n	m_{sat}			$\nu(\text{CO})/\text{cm}^{-1}$	
	this work	ref 14	ref 17	$\text{Au}_n(\text{CO})_{m,\text{sat}}^-$	$\text{Au}_n(\text{CO})^-$
2			2		
3	$\geq 1^b$		2		1995
4	4		3	1957	
5	4	4	4	2003	
6	6	4		1990	
7	4 ^c			2036	2045
8	4 ^c	5		2028	2045
9	6 ^c	6		2032	2053
10	6 ^d	6		2028	2062
11					2070
12					2053
13					2078
14					2062

^a The absolute uncertainties of the reported frequencies are on the order of $\pm 10\text{ cm}^{-1}$. ^b This is the largest complex we observe for Au_3^- but saturation may not have been established yet, even at the highest CO pressures used in the experiment. ^c Intermediate saturation. Further, slower CO addition is observed at high $p(\text{CO})$. ^d Further CO addition may occur at high $p(\text{CO})$ but is masked by congestion in the mass spectrum.

addition can go on, leading to additional, but less pronounced signals for some higher complexes. The highest coverage is observed at $\text{Au}_7(\text{CO})_5^-$, $\text{Au}_8(\text{CO})_7^-$, and $\text{Au}_9(\text{CO})_7^-$, although the assignment becomes difficult for complexes containing 7 or more CO molecules due to overlap in the mass spectra.

The lower trace in Figure 1 illustrates the changes in the mass spectrum if the complexes are irradiated with IR light that is in resonance with IR active absorptions in the complexes, i.e., when absorption of multiple IR photons leads to fragmentation characterized by CO loss. By recording the mass spectrometric intensity of a selected complex as a function of the frequency of the IR light, size specific IR-MPD spectra are obtained. These spectra are shown in Figure 2 for selected carbonyl complexes in the $1700\text{--}2200\text{ cm}^{-1}$ range and the peak frequencies, estimated by visual inspection of the spectra, are listed in Table 1. The spectra of the monocarbonyl species were recorded by working at reduced CO pressure. They have poorer signal-to-noise ratios due to the necessity to work at low abundances to avoid distortion of the absorption spectra by depletion of complexes with more than one CO. The absorption bands are in a range that is typical for atop bound carbonyl complexes. The band positions shift slightly with cluster size from about 1957 cm^{-1} for $\text{Au}_4(\text{CO})_4^-$ to 2028 cm^{-1} for $\text{Au}_{10}(\text{CO})_6^-$.

Discussion

High CO Coverage Complexes. High partial pressures of CO result in saturated $\text{Au}_n(\text{CO})_m^-$ complex compositions that are in close agreement with those reported previously by Wallace and Whetten.¹⁴ The reactor aspects of the experiments were quite similar and, like them, we estimate pressures of several tens of Torr in the reactor channel and residence time of tens of microseconds. The reactions are expected to be in the high-pressure limit and are, as they discuss, likely under equilibrium control. Small differences between our results and those of Wallace and Whetten are the following: (i) we observe formation of the Au_3CO^- complex (Au_3^- appeared unreactive under their conditions); (ii) we observe saturation of $\text{Au}_6(\text{CO})_m^-$ at $m = 6$ and not at $m = 4$; and (iii) we observe some further addition of CO to the saturated complexes at very high $p(\text{CO})$

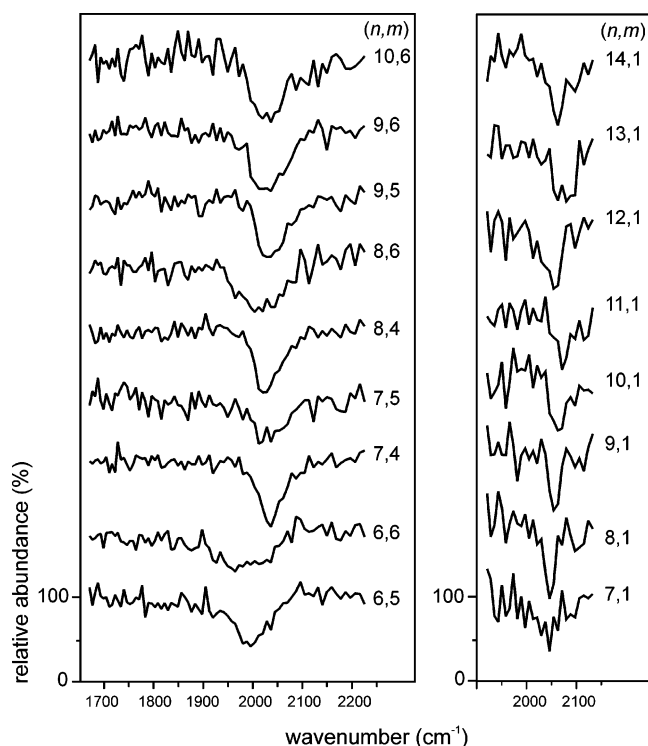


Figure 2. IR multiple photon dissociation spectra of anionic gold cluster carbonyls, $\text{Au}_n(\text{CO})_m^-$.

for $n \geq 7$. Such small differences are not surprising, as both experiments use a second pulse valve to introduce the CO and it is difficult to quantify $p(\text{CO})$ as well as the reaction time in this situation; it might well be that our experimental setup allows higher maximum $p(\text{CO})$ values and/or longer reaction times. Both experiments conclude that $\text{Au}_5(\text{CO})_4^-$, $\text{Au}_7(\text{CO})_4^-$, $\text{Au}_8(\text{CO})_4^-$, $\text{Au}_9(\text{CO})_6^-$, and $\text{Au}_{10}(\text{CO})_6^-$ show (intermediate) saturation and our study adds $\text{Au}_4(\text{CO})_4^-$ and $\text{Au}_6(\text{CO})_6^-$ to this list. The Au_3CO^- complex that we observe is not necessarily a saturated complex and higher $p(\text{CO})$ might result in further CO addition. In this regard we note that $\text{Au}_3(\text{CO})_2^-$ has been observed as the saturated product following addition of CO to Au_3^- in an ion trap²⁰ and that the same species has been identified as the saturated chemisorption product by PES.¹⁷ The PES study is also in agreement with our saturation of $\text{Au}_5(\text{CO})_m^-$ at $m = 4$ but differs in finding $m = 3$ rather than 4 for $\text{Au}_4(\text{CO})_m^-$.

The underlying mechanisms that determine saturation coverages remain unclear in the case of the anions. Wallace and Whetten discussed electron counting rules but came to no clear conclusions.¹⁴ We have recently shown in a study of cationic $\text{Au}_n(\text{CO})_m^+$ complexes with $n \leq 10$ that CO saturation coverages can be attributed to geometric effects that determine the number of available active sites.¹¹ In that study, the observed saturation behavior is in agreement with the structures of Au_n^+ clusters determined by ion mobility studies in combination with DFT calculations.²² Similar information is now available for the anionic clusters.²¹

The structures of Au_n^- ($n = 3$ –10) as determined from ion mobility measurements are shown in Figure 3. From the studies of CO saturation of cationic clusters three rules have been derived for the CO binding to the gold atoms: (i) CO binds only to gold atoms with coordination up to 4, (ii) each gold atom can accommodate at the most one CO ligand, and (iii) gold atoms in the center of planar clusters are unreactive (including four-coordinated sites such as that found in the center of the X-shaped isomer of Au_5^+).¹¹ If applied analogously to

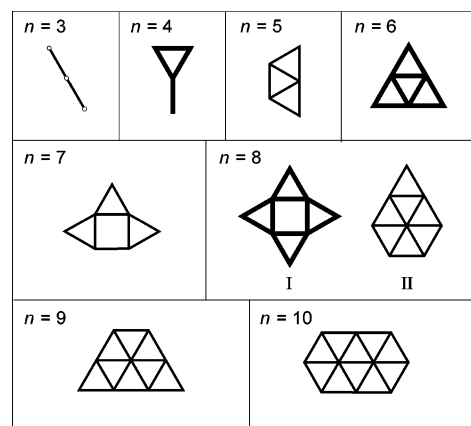


Figure 3. Ground-state structures of Au_n^- anionic clusters from ref 21 as identified by ion mobility measurements, vertical electron detachment energies, and DFT calculations. These experiments cannot distinguish between two possible structures of Au_8^- and both are shown. The structures shown in bold identify the structures deduced from this study.

the anions, these rules predict from the ion mobility structures the following saturation compositions of $\text{Au}_4(\text{CO})_4^-$, $\text{Au}_5(\text{CO})_5^-$, $\text{Au}_6(\text{CO})_6^-$, $\text{Au}_7(\text{CO})_5^-$, $\text{Au}_8(\text{CO})_4^-$ (structure I), and $\text{Au}_8(\text{CO})_7^-$ (structure II). For structure I Au_8^- it is assumed that the four-coordinated edge sites are similar to the central atom of the X-shaped isomer of Au_5^+ and also do not bind CO. Out of those compositions we identify experimentally $\text{Au}_4(\text{CO})_4^-$, $\text{Au}_6(\text{CO})_6^-$, $\text{Au}_8(\text{CO})_4^-$, and $\text{Au}_8(\text{CO})_7^-$ as (intermediate) saturation compositions of anionic carbonyls. In agreement with the PES result of Zhai and Wang¹⁷ we identify $\text{Au}_5(\text{CO})_4^-$ rather than $\text{Au}_5(\text{CO})_5^-$ as the saturation composition when $n = 5$. To rationalize this composition on a geometric basis, the binding rules would have to be revised to preclude binding at the four-coordinated edge site, as proposed by Zhai and Wang; however, this cannot be general for the anions as such sites are occupied in, for example, $\text{Au}_6(\text{CO})_6^-$.

In the case of the cations there is evidence that successive CO addition can result in a change in the cluster structure to accommodate more CO. An indication for such reorganization is found for the carbonyls of Au_8^+ : at intermediate CO pressure $\text{Au}_8(\text{CO})_4^+$ shows a pronounced intensity, but at higher $p(\text{CO})$ CO addition goes on to form $\text{Au}_8(\text{CO})_7^+$. This transition would be consistent with a reorganization of the Au_8 cluster core from structure I to structure II. A similar effect is found for the saturation of the cation $\text{Au}_8(\text{CO})_m^+$ at $m = 7$ that is thought to be due to the gold cluster reorganizing to adopt the same planar structure (II). For other cluster sizes we find no evidence for such reorganization.

For several cluster sizes the observed saturation compositions, e.g., $\text{Au}_7(\text{CO})_4^-$, $\text{Au}_9(\text{CO})_6^-$, or $\text{Au}_{10}(\text{CO})_6^-$, cannot be explained on the basis of the bare cluster structures. Inspection of the low-lying excited-state geometries discussed by Furche et al.²¹ shows no obvious candidate structures either. It is particularly hard to rationalize the saturation of Au_7^- at $m = 4$ in terms of available binding sites. For this cluster there are no low-energy isomers, the ground-state structure shown in Figure 3 lies 0.5 eV below the next highest energy structure. In conclusion, for the anionic carbonyls we find a correlation between geometric structure and the saturation number, m_{sat} , for some clusters only and the saturation behavior does not seem to be a general tool for structure analysis for those clusters.

From the IR spectra of the high-coverage $\text{Au}_n(\text{CO})_m^-$ complexes given in Figure 2 we find that $\nu(\text{CO})$ is in the range from 1950 to 2030 cm^{-1} (Table 1). In all cases the $\nu(\text{CO})$ value

is indicative of CO bound atop, μ^1 , to a single Au atom and we find no evidence for μ^2 - or μ^3 -bridge-bound CO. The changes of $\nu(\text{CO})$ with charge, size, and coverage can be understood in terms of how CO binds and are discussed below. In addition we find no evidence for the dimerization of CO on the cluster surface to form a “glyoxylate”, $-\text{C}(=\text{O})-\text{C}(=\text{O})-$, species. This possibility has been raised in response to the observation that the saturated $\text{Au}_n(\text{CO})_m^-$ compositions favor even numbers of CO ligands.¹⁴ We can rule this out, as such a species is expected to absorb well below the observed values of $\nu(\text{CO})$ ($\nu(\text{CO})$ in glyoxal is at 1745 cm^{-1}).

We do not resolve structure in the $\nu(\text{CO})$ bands, although all the bands are wider than the IR laser bandwidth ($\sim 20\text{ cm}^{-1}$). Single, narrow peaks are indicative of the CO ligands occupying equivalent or similar sites in the saturated complexes. Thus the relatively narrow peak observed for $\text{Au}_8(\text{CO})_4^-$ is consistent with CO binding at the 4 apex atoms of structure I shown in bold in Figure 3. The $\text{Au}_7(\text{CO})_4^-$ complex also shows a narrow peak; however, there is no obvious structural candidate for this stoichiometry, adding to the puzzle this complex presents. The $\text{Au}_6(\text{CO})_6^-$ complex has a broad absorption extending from 2050 to 1900 cm^{-1} . The corresponding cationic complex, $\text{Au}_6(\text{CO})_6^+$, exhibits a similar extended $\nu(\text{CO})$ absorption, but resolved into two peaks that we attributed to CO adsorbed at the apex atoms of the triangular structure shown for $n = 6$ in Figure 3 and at the 4-fold coordinated edge sites.¹¹ This pattern appears to be repeated for the anionic complex, reinforcing the stoichiometric argument and indicating that the anion adopts the same triangular structure.

Dependence of $\nu(\text{CO})$ on Coverage. In surface studies, the coverage dependence of the CO stretching frequency can often be described in terms of the Blyholder model. There, an increase of the number of the adsorbed CO molecules leads to competition for the electrons available for back-donation from the metal, effectively reducing the occupancy of the antibonding π^* orbitals of the CO ligands and increasing the $\nu(\text{CO})$ frequency. Such a dependence on coverage is observed for CO adsorbed on most transition metal surfaces, in coordination compounds, and also in the carbonyls of neutral rhodium clusters where the $\nu(\text{CO})$ bands are slightly blue-shifted with increasing number of CO molecules.¹⁰

However, for CO interacting with gas-phase gold clusters a different dependence is found. For the carbonyls of anionic and cationic gold clusters we find that the $\nu(\text{CO})$ frequencies slightly decrease with coverage (Figure 4). The shift varies with cluster size, and is usually on the order of $\sim 4\text{ cm}^{-1}$ per CO molecule. A similar effect is observed for CO adsorbed on gold surfaces. There, the shift is interpreted in terms of two contributing mechanisms, the “chemical shift”, i.e., the effect of the metal–CO binding on $\nu(\text{CO})$, and the dipolar coupling of CO ligands. These contributions affect $\nu(\text{CO})$ in opposite directions, with the chemical shift being dominating overall.²³ A negative chemical shift corresponds to a weakening of the CO bond with increasing coverage that points to deviations from the Blyholder model. In fact, for cationic gold clusters, the d-type orbitals are low in energy relative to the π^* orbitals of the CO making any $\text{Au} \rightarrow \pi^*$ interaction weak.² Therefore, back-donation is much less important for the binding compared to the earlier transition metals and donation from the 5σ orbital is the more important contribution to CO bonding to Cu, Ag, and Au centers. In most transition metal complexes the shift of $\nu(\text{CO})$ is dominated by π^* -back-donation and insensitive to the degree of σ -donation.²⁴ However, when the contribution of π^* -back-donation is low, as in the case of gold, small effects related to the amount of

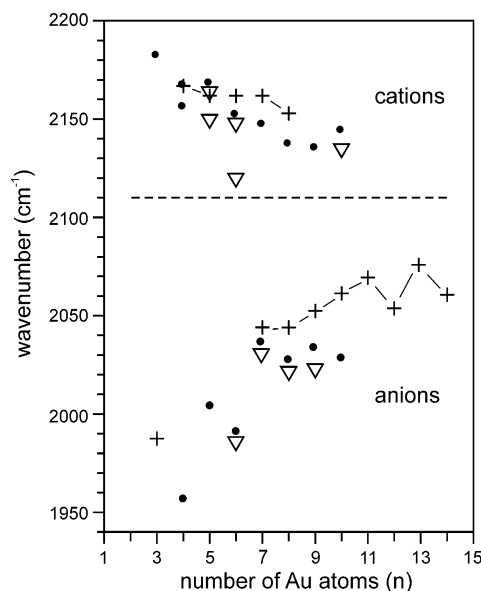


Figure 4. Comparison of the values of $\nu(\text{CO})$ for anionic and cationic gold cluster carbonyls, $\text{Au}_n(\text{CO})_m^\pm$, as a function of cluster size, n , and CO uptake, m . The monocarbonyl complexes ($m = 1$) are represented by joined + symbols and the saturated complexes by solid circles. The saturated stoichiometries, as given by (n, m) , are (4,4), (5,4), (6,6), (7,4), (8,4), (9,6), and (10,6) for the anions and (3,3), (4,4), (5,4), (6,5), (7,6), (8,7), (9,8), and (10,6) for the cations. In the cases of intermediate saturation the higher complexes formed at high $p(\text{CO})$ are represented by open triangles (∇). For complexes with several absorption features, all values are depicted. The absolute uncertainties of the values are typically $\pm 10\text{ cm}^{-1}$, but relative shifts can be determined more precisely. The dashed line indicates the $\nu(\text{CO})$ value for CO adsorbed on gold surfaces.

σ -donation can be observed. The 5σ orbital may be slightly antibonding in the CO bond and a lower amount of donation for increasing coverage, associated with competition for acceptor orbitals, would explain the observed negative shifts.²³

Dependence of $\nu(\text{CO})$ on Cluster Size. As seen in Figure 4, $\nu(\text{CO})$ increases with cluster size, n , for both the monocarbonyl as well as the saturated $\text{Au}_n(\text{CO})_m^-$ complexes. This trend can be largely understood in terms of charge dilution. The negative charge decreases the CO bond strength and hence $\nu(\text{CO})$ via two mechanisms. First, the negative charge is available for back-donation, and second, there is an electrostatic effect that lowers $\nu(\text{CO})$ through the interaction of the CO dipole with the nearby negative charge. In the case of the cations we estimated the electrostatic contribution by calculating the electric field at the CO and using data from the model calculations of Goldman and Krough-Jespersen²⁴ to predict the frequency shift relative to free CO. Assuming charge is shared among the cluster metal atoms, this model predicts that $\nu(\text{CO})$ should drop by $\sim 15\text{ cm}^{-1}$ when going from $n = 3$ to 10. The effect should be reversed for anionic clusters and $\nu(\text{CO})$ should rise by a similar amount over the same range. The measured shift over the same range is 80 cm^{-1} , implying that π^* -back-donation is the main factor for lowering $\nu(\text{CO})$ in small anionic gold clusters. The available electron density at individual binding sites decreases as the cluster size increases, i.e., the charge is diluted. We expect both the anion and the cation frequencies to converge to the $\nu(\text{CO})$ value of CO adsorbed on gold surfaces of $\sim 2110\text{ cm}^{-1}$,⁷ which appears to be the case. This convergence is not symmetrical around the bulk value for the cations and the anions, being larger for the small anionic complexes where π^* -back-bonding may have a larger contribution.

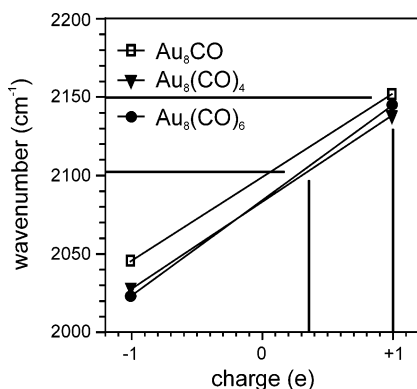


Figure 5. Plot relating $\nu(\text{CO})$ to charge for carbonyls of Au_8 . Horizontal lines mark the values of $\nu(\text{CO})$ for CO on deposited Au_8 particles on defect-rich MgO (lower line) and defect-poor MgO (upper line) taken from ref 4 after conversion from $\nu(^{13}\text{CO})$ to $\nu(^{12}\text{CO})$. The vertical lines mark the corresponding partial charges. It is assumed that the deposited particles are highly covered with CO.

Dependence of $\nu(\text{CO})$ on the Charge State. Although there are noticeable deviations from the standard picture of carbonyl bonding to open-shell transition metals for the gold cluster carbonyls, the observed dependence of $\nu(\text{CO})$ on the cluster charge (Figure 4) is similar to the one observed in other metal systems. The CO bond is significantly weakened in the anions compared to the cationic complexes, with shifts between the two charge states of $\nu(\text{CO})$ of about 200 cm^{-1} for the smallest clusters investigated ($n = 3$) to about 100 cm^{-1} for cluster sizes around $n = 10$. Nevertheless, these charge dependent shifts are $\sim 20\%$ less than in the case of Rh cluster carbonyls.¹⁰

There are recent measurements of low-temperature matrix IR spectra of co-deposited Au and CO that are believed to contain spectral features of monocarbonyls of small neutral gold clusters, Au_nCO ($n = 1\text{--}5$).²⁵ Most of the assigned $\nu(\text{CO})$ values fall between our values for the anionic and cationic complexes and accordingly could be assigned to atop-bound CO in neutral complexes. A feature observed at 1853 cm^{-1} is suggested to be due to μ^2 -bound CO on Au_5 . The μ^2 -binding of CO to neutral Au_5 is recurring in some theoretical studies.^{25–27} We do not find any signature for μ^2 -bound CO on any anionic or cationic cluster, however. Independent DFT calculations performed on the cationic, anionic, and neutral monocarbonyl complexes, $\text{Au}_n\text{CO}^{+/0/-}$ for $n = 1$ to 6, are consistent with our observed dependence of $\nu(\text{CO})$ on both the charge state and the cluster size.²⁸

Implications for the Charge State of Supported Clusters. Figure 5 shows a more detailed plot of the changes in $\nu(\text{CO})$ for the carbonyls of Au_8 depending on the charge state and coverage. Interpolation between the values of anionic and cationic complexes predicts a $\nu(\text{CO})$ of 2080 cm^{-1} for the neutral clusters. This is relatively close to the values for CO adsorbed on bulk Au surfaces (2110 cm^{-1}).

Infrared spectra of CO coadsorbed with O_2 on size-selected deposited Au_8 clusters on MgO have been recently reported by Heiz and co-workers.⁴ They measure different values of $\nu(^{13}\text{CO})$ depending on if the ^{13}CO is adsorbed on clusters deposited on defect-rich (2049 cm^{-1}) or defect-free MgO (2102 cm^{-1}). These numbers correspond to frequencies of 2096 and 2150 cm^{-1} when converted to $\nu(^{12}\text{CO})$. Using the isolated cationic and negatively charged carbonyls of Au_8 as a reference (Figure 5), partial charges of $+0.2\text{ e}$ and $+1\text{ e}$ (or even higher) are obtained. At first sight these values do not agree with a negative polarization of the gold clusters as proposed. However, on the defect-rich surface, where the gold particles are believed

to interact with an electron-donating F-center, the $\nu(\text{CO})$ value is certainly lower than on the defect-free surface, implying a cluster with a higher electron density. One possible interpretation for the observation of apparently positively charged clusters on a negatively charged defect might be the presence of O_2 coadsorbed on these species. The O_2 withdraws electron density from the cluster and gets formally reduced to a superoxide (O_2^-) or peroxide (O_2^{2-}) species. Thereby the O–O bond is weakened and activated. Heiz et al.⁴ assign a band at about 1300 cm^{-1} to this oxygen species that lies somehow between typical values for superoxides ($\sim 1150\text{ cm}^{-1}$) and for free molecular oxygen (1555 cm^{-1}). This binding of O_2 to an initially negatively polarized cluster can explain a decrease of electron density on the metal particle that then effects the CO binding.

Conclusion

In conjunction with our earlier work on the cations an overall picture emerges for the charge and size dependence of the properties of charged gold cluster carbonyl complexes. Clusters of both charge states show saturation CO coverages that are low compared to those observed for open-shell transition metal complexes, consistent with the picture that only low-coordinated gold atoms can act as CO chemisorption sites, and that each site can only accommodate a single CO ligand. This is supported by the vibrational spectroscopy of the complexes, where $\nu(\text{CO})$ is always found to be characteristic of μ^1 , atop binding, regardless of charge or coverage.

The direct correlation between saturation coverage and cluster structure found for cations is not so apparent in the case of the anions. The anion complexes that do not follow the cation binding rules accommodate even fewer CO molecules, implying that even more restrictive binding rules can operate for certain anionic complexes. For both charge states we find evidence that CO addition can promote structural change in the gold cluster structure. This is consistent with the DFT calculations that identify several low-lying isomers for almost all Au clusters, irrespective of charge.

In contrast to what is known for most other transition metal carbonyls, we observe a red-shift of $\nu(\text{CO})$ with increasing CO coverage of the clusters. This is an indication that π^* -back-donation only makes a minor contribution to the Au–CO binding, especially in the case of the cations. With increasing size the anion and the cation frequencies converge to the $\nu(\text{CO})$ value of CO on gold surfaces. The shifts relative to the surface value are not symmetrical pointing to larger π^* -back-bonding in the smaller anionic complexes.

We have discussed the application of charge-dependent measurements of $\nu(\text{CO})$ in the gas phase to calibrate $\nu(\text{CO})$ as a probe of the charge state of deposited clusters. When using this approach, one must be aware that the situation of a cluster on a surface is far more complex than that in the gas phase. Gas-phase structures may not be maintained on the surface, their symmetries are reduced, the surface may sterically hinder CO adsorption, and charge distributions in the cluster may be different due to site-specific cluster–surface interactions. Nevertheless, the gas-phase measurements can form a baseline to gauge the influence of the support. In the case of CO adsorbed on MgO supported Au_8 they point to a positive charge on the cluster, even when it is adsorbed at a defect thought to provide negative charge. This is presumably the effect of coadsorbed O_2 . It would be interesting to study the adsorption of CO on the same particles without coadsorbed O_2 to probe the initial charge state of the clusters. It will also be interesting to study the vibrational spectroscopy of gold cluster CO– O_2 co-

complexes and to check if the negative polarization is the key for the activation of the dioxygen in the catalytic process.

Acknowledgment. We gratefully acknowledge the support by the “Stichting voor Fundamenteel Onderzoek der Materie” (FOM) in providing beam time on FELIX and the skillfull assistance of the FELIX staff, in particular Dr. A. F. G. van der Meer and Dr. B. Redlich.

References and Notes

- (1) Haruta, M.; Yamada, N.; Kobayashi, T.; Iijima, S. *J. Catal.* **1989**, *115*, 301.
- (2) Bernhardt, T. M. *Int. J. Mass Spectrom.* **2005**, *243*, 1.
- (3) Sanchez, A.; Abbet, S.; Heiz, U.; Schneider, W.-D.; Häkkinen, H.; Barnett, R. N.; Landman, U. *J. Phys. Chem. A* **1999**, *103*, 9573.
- (4) Yoon, B.; Häkkinen, H.; Landman, U.; Wörz, A. S.; Antonietti, J.-M.; Abbet, S.; Judai, K.; Heiz, U. *Science* **2005**, *307*, 403.
- (5) Boccuzzi, F.; Chiorino, A.; Manzoli, M. *Surf. Sci.* **2000**, *454–456*, 942.
- (6) Lemire, C.; Meyer, R.; Shaikhutdinov, S. K.; Freund, H.-J. *Surf. Sci.* **2004**, *552*, 27.
- (7) Meyer, R.; Lemire, C.; Shaikhutdinov, S. K.; Freund, H.-J. *Gold Bull.* **2004**, *37*, 72.
- (8) Blyholder, G. *J. Phys. Chem.* **1964**, *68*, 2772.
- (9) Frank, M.; Bäumer, M.; Kühnemuth, R.; Freund, H.-J. *J. Phys. Chem. B* **2001**, *105*, 8569.
- (10) Fielicke, A.; von Helden, G.; Meijer, G.; Pedersen, D. B.; Simard, B.; Rayner, D. M. *J. Phys. Chem. B* **2004**, *108*, 14591.
- (11) Fielicke, A.; von Helden, G.; Meijer, G.; Pedersen, D. B.; Simard, B.; Rayner, D. M. *J. Am. Chem. Soc.* **2005**, *127*, 8416.
- (12) Lee, T. H.; Ervin, K. M. *J. Phys. Chem.* **1994**, *98*, 10023.
- (13) Balteanu, I.; Balaj, O. P.; Fox, B. S.; Beyer, M. K.; Bastl, Z.; Bondybey, V. E. *Phys. Chem. Chem. Phys.* **2003**, *5*, 1213.
- (14) Wallace, W. T.; Whetten, R. L. *J. Phys. Chem. B* **2000**, *104*, 10964.
- (15) Wallace, W. T.; Whetten, R. L. *Eur. Phys. J. D* **2001**, *16*, 123.
- (16) Wallace, W. T.; Wyrwas, R. B.; Leavitt, A. J.; Whetten, R. L. *Phys. Chem. Chem. Phys.* **2005**, *7*, 930.
- (17) Zhai, H.-J.; Wang, L.-S. *J. Chem. Phys.* **2005**, *122*, 051101.
- (18) Fielicke, A.; von Helden, G.; Meijer, G.; Simard, B.; Dénommée, S.; Rayner, D. M. *J. Am. Chem. Soc.* **2003**, *125*, 11184.
- (19) Oepts, D.; van der Meer, A. F. G.; van Amersfoort, P. W. *Infrared Phys. Technol.* **1995**, *36*, 297.
- (20) Hagen, J.; Socaciu, L. D.; Heiz, U.; Bernhardt, T. M.; Wöste, L. *Eur. Phys. J. D* **2003**, *24*, 327.
- (21) Furche, F.; Ahlrichs, R.; Weis, P.; Jacob, C.; Gilb, S.; Bierweiler, T.; Kappes, M. M. *J. Chem. Phys.* **2002**, *117*, 6982.
- (22) Gilb, S.; Weis, P.; Furche, F.; Ahlrichs, R.; Kappes, M. M. *J. Chem. Phys.* **2002**, *116*, 4094.
- (23) France, J.; Hollins, P. J. *Electron Spectrosc. Relat. Phenom.* **1993**, *64/65*, 251.
- (24) Goldman, A. S.; Krogh-Jespersen, K. *J. Am. Chem. Soc.* **1996**, *118*, 12159.
- (25) Jiang, L.; Xu, Q. *J. Phys. Chem. A* **2005**, *109*, 1026.
- (26) Phala, N. S.; Klatt, G.; van Steen, E. *Chem. Phys. Lett.* **2004**, *395*, 33.
- (27) Fernández, E. M.; Ordejón, P.; Balbás, L. C. *Chem. Phys. Lett.* **2005**, *408*, 252.
- (28) Wu, X.; Senapati, L.; Nayak, S. K.; Selloni, A.; Hajaligol, M. J. *Chem. Phys.* **2002**, *117*, 4010.